FAST TRACK COMMUNICATION

The decay of the C 1s → 2π $^3\Pi$ inner-shell excited state of CO

V Feyer[1,2]**, P Bolognesi**[1]**, M Coreno**[1,3]**, K C Prince**[3,4]**, L Avaldi**[1,3]**,
B Jansik**[5] **and V Carravetta**[5]

[1] CNR-IMIP, Area della Ricerca di Roma 1, CP 10, 00016 Monterotondo Scalo, Italy
[2] Institute of Electron Physics, National Academy of Sciences, Uzhgorod, Ukraine
[3] INFM-TASC, Gasphase beamline@Elettra, Area Science Park, 34012 Basovizza, Trieste, Italy
[4] Sincrotrone Trieste, Area Science Park, 34012 Basovizza, Trieste, Italy
[5] CNR-IPCF, Area della Ricerca di Pisa, Via G Moruzzi, 156124 Pisa, Italy

Abstract
Electron impact has been used to excite dipole forbidden inner-shell transitions
of CO which are not accessible by photon impact. Coincidence techniques
have then been used to study the decay of the C $1s^{-1}2p\pi$ $^3\Pi$ inner-shell excited
state, and to isolate this autoionization spectrum from that of the $^1\Pi$ inner-
shell excited state. An *ab initio* multiconfiguration and multicentre calculation
allowed the assignment of the spectral features to the various participator
and spectator transitions leading to the final CO$^+$ doublet and quartet states.
Although the same doublet states are populated from both the singlet and triplet
intermediate states, the experimental intensities and energies are significantly
different due to Franck–Condon effects.

With the advent of highly intense undulator sources and new monochromators, the decay
of inner-shell resonantly excited states in molecules has been studied in great detail in
diatomic and small polyatomic molecules [1]. The different decay processes have been
used to understand the nature of the core hole excited states and to investigate states of the
cation not directly accessible by direct photoionization. The high resolution achieved has
allowed the observation and investigation of basic processes such as energy dispersion and
narrowing of the lineshapes, due to energy conservation [2], lifetime interference effects [3],
the Doppler effect in the ejected electron spectra [4] as well as ultrafast dissociation [5]. All
these studies involved only the decay of inner-shell excited states populated by dipole-allowed
transitions. Only recently the excitation of a dipole forbidden transition in He by photons has
been observed by measuring the forward–backward asymmetry of the photoelectron angular
distribution [6]. On the other hand it is well known that 'dark' states (in optical terminology)
populated via dipole forbidden transitions can be accessed in electron impact experiments
and that the contribution of such transitions in electron energy loss (EELS) spectra can be
enhanced either by increasing the momentum transfer in the collision or by lowering the
incident energy. Several years ago Ungier and Thomas [7] combined the detection of the

inelastically scattered electrons, which had suffered an energy loss equal to an inner-shell excitation, with the simultaneous detection of the electrons ejected in the decay of the excited state. This coincidence technique is a unique tool which can be applied to characterize the decay of inner-shell dipole forbidden states. However those authors limited their study to the decay of dipole allowed transitions. Here we have taken advantage of the high detection efficiency of an electron–electron multicoincidence set-up, equipped with ten independent electron analysers and used this technique for the study of the decay of both the dipole allowed singlet, and dipole forbidden triplet, C 1s → 2π $^{1,3}\Pi$ excited states in CO.

CO, one of the simplest diatomic molecules, was chosen because on the one hand its autoionization spectrum displays all the complexity of final states with one hole in the valence shells (participator states) or with two holes in the valence shells and one particle in an initially empty orbital (spectator states) [1]. On the other hand CO has few enough electrons to be amenable to *ab initio* electronic structure calculations.

From the decay of the $^3\Pi$ excited state, one may expect that the same final doublet CO^+ states reached by the decay of the $^1\Pi$ excited state are populated. However the relative intensity may differ depending on the difference in the potential curves of the two excited states and on the difference in the autoionization decay rates, determined by Coulomb coupling. In addition also the quartet CO^+ states, not directly accessible by other experimental techniques can be populated by decay of the $^3\Pi$ excited state, but not from the $^1\Pi$ excited state. The decay spectra of inner-shell excited states are usually named '*autoionization*' spectra in the electron impact experiments, while they are referred as '*resonant Auger*' spectra in synchrotron spectroscopy due to the typical resonant condition needed for their observation. In the following the spectra measured in this work will be referred as '*autoionization*' spectra, while in the reference to the literature the conventional nomenclature depending on the excitation source will be used.

The measurements were performed using the multicoincidence end-station of the gas phase beamline at Elettra storage ring [8], which was equipped with an electron gun (EKF 300, Omicron GmbH) for these measurements. The scattering chamber hosts ten independent electrostatic analysers, arranged in groups of three and seven analysers and placed at 30° from each other. They are mounted on two separate turntables in a plane perpendicular to the incident beam (i.e. at 90° with respect to the direction of the incident beam). The inelastic scattered electrons, after suffering an energy loss of 287.4 or 285.95 eV for the excitation of C $1s^{-1}2\pi$ $^{1,3}\Pi$ states respectively, were detected by the three analysers of the small turntable. The ejected autoionization electrons in the range 256–276 eV were detected by the seven analysers mounted on the bigger turntable. The energy resolution and the angular acceptance in the dispersion plane of the spectrometers were $\Delta E_{1,2} = 0.8$ eV and $\Delta\vartheta_{1,2} = \pm 3°$. The coincidence electronics consists of three independent time-to-digital converters (TDC). In the experiment each TDC unit is operated in the common start mode with the signals of each one of the three analysers of the small turntable used as starts and the signals from the other seven as stops. In this way 21 coincidence pairs are collected simultaneously. All the experimental settings and the data acquisition are controlled via a PC equipped with NI-LabView® software. The same software monitors the stability of the set-up during the long acquisition times of the coincidence scans via the measurement of the non-coincidence count rates of the ten analysers at fixed time intervals [9]. The coincidence signals of the 21 scattered-ejected pairs were summed, after a careful energy calibration of the non-coincidence autoionization spectra independently collected by the seven analysers. This provision enhances the overall efficiency of our set-up of a factor 20 with respect to the usual coincidence apparatus equipped with two analysers. The kinetic energy scale of the different analysers was established by measuring the C 1s Auger spectrum in the region of the CO^{2+} B state [10]. Under typical experimental
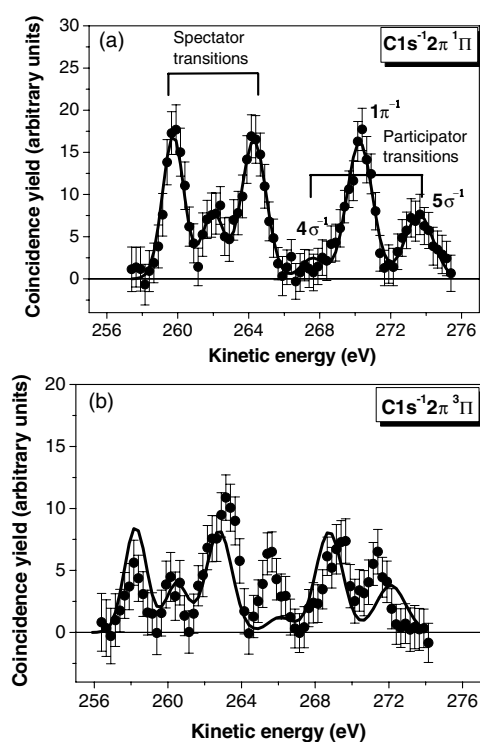
Figure 1. The autoionization spectra following the excitation of the C $1s^{-1}2\pi$ $^1\Pi$ (a) and $^3\Pi$ (b) states. The two different inner-shell excited states have been selected by measuring in coincidence inelastically scattered electrons, which suffered an energy loss of 287.4 or 285.95 eV respectively, and the ejected electrons. The full line in (a) is a fit to the experimental data using literature values [14, 15] for the participator and spectator transitions convoluted with the present energy resolution. The full line in (b) is the same as in (a) appropriately rescaled to account for the different excitation probability of the $^3\Pi$ state and shifted by 1.5 eV, the spin orbit splitting between the two inner-shell excited states.

conditions of about 1×10^{-5} mbar of gas pressure and 1.8 μA incident current, acquisition times of about 6–10 hours/point were needed in order to achieve an acceptable statistics in the coincidence measurements.

The autoionization spectra measured at 600 eV incident energy in coincidence with inelastically scattered electrons which suffered an energy loss equal to the excitation of the C $1s^{-1}$ 2π $^{1,3}\Pi$ states are shown in figures 1(a) and (b), respectively. This incident energy has been chosen because at 600 eV a triplet/singlet ratio of about 0.6 has been measured [11, 12] and the spectral features due to the energy loss and the decay can be easily separated. Moreover the chosen kinematics is characterized by a momentum transfer ($\sim$8 au) which also enhances the excitation of the $^3\Pi$ state. Finally at this energy the final state effects (post collision interaction) can be neglected because the scattered electron is faster than the ejected one [13].

The spectra (figure 1) are characterized in the high kinetic energy part by features due to the participator decay and in the low kinetic energy part by the manifolds of spectator transitions. In CO the participator transitions populate the lowest three CO$^+$ states, i.e. $5\sigma^{-1}$ $^2\Sigma^+$, $1\pi^{-1}$ $^2\Pi$ and $4\sigma^{-1}$ $^2\Sigma^+$, while by spectator decay several final states with two holes in the valence orbitals and an electron in the 2π orbital are populated.

High-resolution photon excited data and accurate theoretical analysis of the decay spectrum of the C $1s^{-1}2\pi$ $^1\Pi$ state exist in the literature [14, 15]. This information has been used in the analysis of the coincidence spectrum reported in figure 1(a). A reasonable representation of the spectrum is achieved by convoluting the literature data with the present energy resolution. The main difference with the resonant Auger spectra measured by photon excitation is the relative intensity of the $4\sigma^{-1}$ $^2\Sigma^+$ state, which in the present measurement is smaller than in those data. The feature observed at about 262 eV in the coincidence spectrum can be assigned [14, 15] to spectator transitions to the CO$^+$ $2^2\Sigma^-$ and $2^2\Delta$ final states. This feature was observed in the high energy non-coincidence spectrum by Ungier and Thomas [7], but not in the coincidence spectrum with inelastically scattered electrons of 287.4 eV loss. This led those authors to conclude that the feature did not originate from the decay of the inner-shell excited state. The present observation and its presence in the resonant Auger spectra [14, 15] rule out that hypothesis.

The decay spectrum of the C $1s^{-1}2\pi$ $^3\Pi$ state is shown in figure 1(b). The overall intensity of this spectrum is about 0.53 ± 0.08 of that of the singlet excited state. This value is consistent with the ratio observed in the excitation of the two inner-shell excited states in EELS [11, 12]. Thus it can be concluded that the decay rate of the two excited states in this spectral region is almost the same. Our analysis of the spectrum begun with the assumption [7] that most of the features might be assigned by shifting the autoionization spectrum of the singlet state by 1.5 eV, the spin orbit splitting of the inner-shell singlet and triplet excited states [7, 11, 13, 16]. The result of such a procedure is shown in figure 1(b), where the best fit to the spectrum of the $^1\Pi$ state has been rescaled in order to match the intensity of the $1\pi^{-1}$ peak in the spectrum of the $^3\Pi$ state. The comparison shows that, despite the resemblance, the relative position and intensity of the features in the two spectra are different. In order to explain these observations the autoionization spectra of both the $^{1,3}\Pi$ inner-shell excited states have been calculated *ab initio* by using the MCSF method (number of configurations 150 000–250 000) and a large basis set aug-cc-pVTZ [11s, 6p, 3d, 2f | 5s, 4p, 3d, 2f] for the spectral energies and an independent particle SCF method with a large multicentre basis set covering the high energy continuum [17] for the spectral intensities. All the electronic states were first computed at the ground state equilibrium geometry ($R = 2.132$ au), i.e. in the vertical approximation. The energy difference between singlet and triplet $^{1,3}\Pi$ core excited states was found to be 1.6 eV in good agreement with the experimental value of 1.5 eV [7, 11, 13, 16]. The potential surfaces were then computed both for the two core-excited states and for the three participator final states $5\sigma^{-1}$ $^2\Sigma^+$, $1\pi^{-1}$ $^2\Pi$ and $4\sigma^{-1}$ $^2\Sigma^+$ at the same level of computational accuracy in the range $R = 1.6$–5.0 au. For the more CPU demanding calculations of the potential surfaces of the various spectator states, a smaller CAS space was adopted (number of configurations 20 000). It was verified that this reduction, similarly to previous calculations, may affect the absolute energies but it does not change the shape of the potential surfaces. The vibrational states of the ground electronic state, the core-excited and all the considered final electronic states were then obtained by numerical integration of the nuclear Schrödinger equation in the Born–Oppenheimer approximation. The vibrational spectra have been energy shifted in order to take into account the energy difference observed between extended and reduced MCSF calculations in the vertical approximation. The relevant vibrational states of these core excitations are $v = 0$ and 1 for the $^1\Pi$ state and $v = 0$, 1 and 2 for the $^3\Pi$ state in agreement with the analysis of the energy loss spectra by Francis *et al* [11]. All the Franck–Condon (FC) factors ($\geqslant 0.01$) between such CO* states and the vibrational states of each final CO$^+$ participator or spectator electronic state have been considered and weighted by the correspondent computed autoionization rate in order to simulate the decay spectrum. It should be pointed out that the theoretical spectrum could be
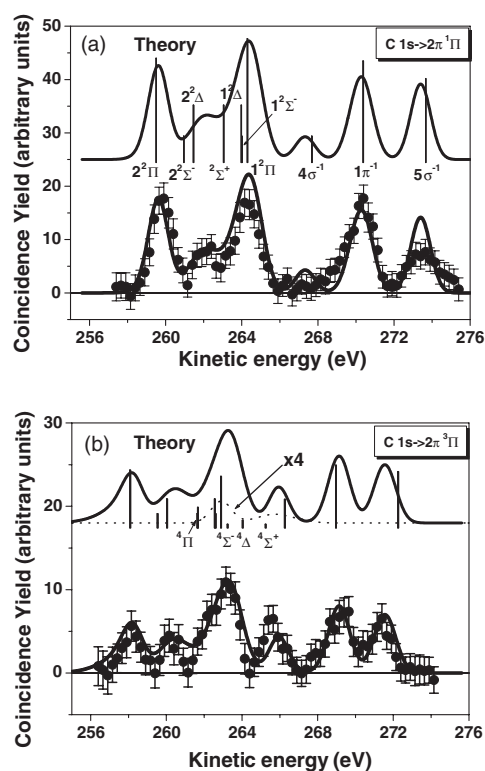
Figure 2. Comparison between the calculated and measured autoionization spectra following the excitation of the C $1s^{-1}2\pi$ $^1\Pi$ (a) and $^3\Pi$ (b) states. The full lines superimposed on the experimental data, also shown in the top panel of both figures, are the calculated spectra. The dotted line in the top panel of (b) is the calculated contribution ($\times 4$) of the decay to CO^+ quartet states. The bar spectra represent the energy and relative intensity of the transitions to the different final states in the vertical approximation. The transitions to the CO^+ doublet final states are labelled only in (a); they appear in the same order, but energy shifted, in (b). In the latter the transitions to the CO^+ quartet final states are indicated.

approximated here as the sum of the several FC factor distributions, neglecting any effect of direct and resonant channel interference and lifetime vibrational interference, only because it was compared to a quite low-resolution experimental spectrum. Indeed, finally the theoretical results had to be convoluted with a Gaussian function of 1.2 eV FWHM that represents the overall experimental resolution, in order to be compared with the experimental spectral profile.

In figures 2 the theoretical calculations are compared with the experimental results. The bar diagrams represent energy position and intensity of the spectrum of the autoionization electrons computed in the vertical approximation. A comparison of the calculated bands of the three participator states $5\sigma^{-1}$ $^2\Sigma^+$, $1\pi^{-1}$ $^2\Pi$ and $4\sigma^{-1}$ $^2\Sigma^+$, with previous high-resolution measurements of the resonant Auger decay of the C $1s^{-1}2\pi$ $^1\Pi$ state (see figure 3, $v = 0$ in [14]), shows that the structure of the vibrational band is well reproduced in terms of intensity distribution for all the three participator states. Moreover the *ab initio* multicentre method [17] used in the present calculations of the resonant Auger decay rates, results in relative intensities in better agreement with the high-resolution spectrum than the spectrum computed by the usual 'one-centre approximation' and presented in figure 5 of the same paper

[14]. The relative energy positions of the three computed participator peaks are in reasonable agreement with the present experimental data. In particular, the calculations reproduce well the general 'shrinking' of the relative positions of the participator peaks going from the 'singlet' (figure 2(a)) to the 'triplet' (figure 2(b)) decay spectra (see for example the shift of the $1\pi^{-1}$ peak towards the $5\sigma^{-1}$ peak). This results from the differences in the potential curves of the triplet and singlet intermediate states. Indeed the triplet state has a less tightly bound potential with a larger equilibrium bond distance and larger Franck–Condon factors for the higher vibrational states [18].

The absolute decay rate calculated for the two inner-shell excited states is the same within a few per cent. This finding is in agreement with the experimental observation. Thus the calculated spectrum of the singlet inner-shell excited state has been rescaled arbitrarily in order to obtain the best overall representation of the experimental spectrum in figure 2(a). Then the same rescaling factor multiplied by the $^3\Pi/^1\Pi$ excitation probability ratio has been used for the comparison between theory and experiment in the case of the triplet inner-shell excited state in figure 2(b).

In the participator part of the spectrum, general agreement between experiment and theory is observed except that theory appears to overestimate the intensity of the $5\sigma^{-1}$ peak in the decay spectrum of the $^1\Pi$ state, and to underestimate the intensity of the $4\sigma^{-1}$ peak in the spectrum of the $^3\Pi$ state. In order to understand whether the CO^+ quartet states have been significantly populated by the decay of the triplet excited state in this energy region, a calculation of the potential energy curves of the lowest quartet states and of the autoionization decay rate to these states from the triplet excited state has been made [18] by the same computational procedure adopted for the doublet final state. Four quartet states, namely $^4\Sigma^+$, $^4\Delta$, $^4\Sigma^-$ and $^4\Pi$, were found between 261 and 265.5 eV (see figure 2(b)). The energies in the vertical approximation of the transitions to these final states are in good agreement with the calculations of Okada and Iwata [19] and Botting and Lucchese [20]. The contribution to the spectrum of the transitions to CO^+ final quartet states is shown as a dotted line in the top panel of figure 2(b). Thus these transitions do contribute to the spectrum in the region of the $4\sigma^{-1}$ peak, but their contribution cannot fully account for the discrepancy observed in the calculated and measured intensity. It should also be noted that the relative intensity of the three features in the participator spectrum of the triplet excited state of the present work is consistent with that observed in the non-coincidence high-resolution work by Almeida *et al* [13].

The analysis of the spectra in the region below 267 eV is less straightforward. Here the three observed bands in the experimental spectrum of the $^1\Pi$ state can be assigned to seven main spectator states. Those with the dominant configurations $5\sigma^{-2}2\pi(1\,^2\Pi)$, $5\sigma^{-1}1\pi^{-1}2\pi(1\,^2\Sigma^-, 1\,^2\Delta, 1\,^2\Sigma^+)$ mainly contribute to the feature at 264.5 eV, while those with configurations $5\sigma^{-1}1\pi^{-1}2\pi(2\,^2\Delta, 2\,^2\Sigma)$ and $4\sigma^{-1}5\sigma^{-1}2\pi(2^2\Pi)$ are responsible for the two features at 262 and 260 eV, respectively. The $^2\Delta$ and $^2\Sigma^-$ states are repulsive and therefore they give rise to broad structureless bands [18]. The $4\sigma^{-1}5\sigma^{-1}2\pi\ (2^2\Pi)$ diabatic state is bound, but in its energy region, around the ground state equilibrium geometry, there are several other $^2\Pi$ states, and consequently several avoided crossings of the adiabatic potential energy curves [18]. The diabatic potential energy curve of the $2^2\Pi$ state runs almost parallel to that of the singlet core-excited state, thus the corresponding FC distribution results in a quite narrow feature that, in reality, would be reasonably smeared out by the interaction with the other diabatic states. We did not consider such subtle effects because the computed FC distribution was in any case convoluted with a broad Gaussian function that simulates the experimental resolution. The calculated spectrum is in agreement with the measured one for both the position and the number of the features. There are small differences in the

relative intensity of the different features in the spectator part of the spectrum and between the spectator and participator parts. The difference in intensity may be due to the independent particle approximation adopted in the *ab initio* calculation of the resonant Auger rates [17]. By this approach, the smallest combinations of determinants, with the appropriate symmetry and spin character, are employed for the description of the electronic states. Of course, the validity of such an approximation may, in principle, be different for the participator and spectator final states, due to the varying strength of electron correlation.

Differently from the case of the singlet spectrum, where all the calculated bands were found to match very well with the measured features in the spectrum, in the case of the spectrum of the $^3\Pi$ excited state (figure 2(b)) we found that the $2^2\Delta$ and $2^2\Sigma^-$ bands had to be shifted by about 0.4 eV in order to match the feature centred at about 260.15 eV in the experimental spectrum. With this shift, the overall shape and the relative intensities of the calculated $^3\Pi$ spectrum are in good agreement with the experiment.

In summary we have taken advantage of the ability of electron impact experiments to populate inner-shell excited states via dipole forbidden transitions, which has no comparable synchrotron radiation technique. Combining a coincidence technique and a high efficiency spectrometer we have made the first observation of the full decay spectrum of the C $1s^{-1}2\pi$ $^3\Pi$ core excited state of the CO molecule. The interpretation and assignment of the experimental results are done via the use of *ab initio* large MCSF calculations for the energies and *ab initio* independent particle multicentre calculations for the intensities. The theoretical results clearly show that the differences in the potential energy surface of the $^3\Pi$ and $^1\Pi$ excited states explain the observed differences of the intensities and energy positions in the spectrum of the participator and spectator peaks. In the calculation of the decay of the $^3\Pi$ excited state, the population of CO^+ quartet states has been taken into account, too. However the contribution of these transitions to the autoionization spectrum has been found to be small. This work shows that despite the poor energy resolution, coincidence measurements of inelastically scattered electrons and Auger electrons are a unique and valuable tool to map the decay of 'dark' states.

References

[1] Svensson S 2005 *J. Phys. B: At. Mol. Opt. Phys.* **38** S821
[2] Kivimäki A, Naves de Brito A, Aksela S, Aksela H, Sairanen O-P, Ausmees A, Osborne S J, Dantas L B and Svensson S 1993 *Phys. Rev. Lett.* **71** 4307
[3] Neeb M, Rubensson J E, Biermann M and Eberhardt W 1994 *J. Electron Spectrosc. Relat. Phenom.* **67** 261
[4] Björneholm O *et al* 2000 *Phys. Rev. Lett.* **84** 2826
[5] Björneholm O, Sundin S, Svensson S, Marinho R R T, Naves de Brito A, Gel'mukhanov F and Ågren H 1997 *Phys. Rev. Lett.* **79** 3150
[6] Krässig B, Kanter E P, Southworth S H, Guillemin R, Hemmers O, Lindle D W, Wehlitz R and Martin N L S 2002 *Phys. Rev. Lett.* **88** 203002
[7] Ungier L and Thomas T D 1983 *Chem. Phys. Lett.* **96** 247

[8] Blyth R R *et al* 1999 *J. Electron Spectrosc. Relat. Phenom.* **101–103** 959
[9] Bolognesi P, Coreno M, Alberti G, Richter R, Sankari R and Avaldi L 2004 *J. Electron. Spectrosc. Relat. Phenom.* **141** 105
[10] Feyer V, Bolognesi P, Coreno M, Prince K C, Avaldi L, Storchi L and Tarantelli F 2005 *J. Chem. Phys.* **123** 224306
[11] Francis J T, Kosugi N and Hitchcock A P 1994 *J. Chem. Phys.* **101** 10429
[12] Feyer V, Bolognesi P, Coreno M, Prince K C and Avaldi L 2007 *Radiat. Phys. Chem.* **76** 450
[13] Almeida D P, Dawber G, King G C and Palásthy B 1999 *J. Phys. B: At. Mol. Opt. Phys.* **32** 3157
[14] Piancastelli M N, Neeb M, Kivimaki A, Kempgens B, Köppe H M, Maier K, Bradshaw A M and Fink R F 1997 *J. Phys. B: At. Mol. Opt. Phys.* **30** 5677
[15] Kukk E, Bozek J D, Cheng W-T, Fink R F and Wills A A 1999 *J. Chem. Phys.* **111** 9642
[16] Shaw D A, King G C, Cvejanovic D and Read F H 1984 *J. Phys. B: At. Mol. Phys.* **17** 2091
[17] Carravetta V, Agren H, Vahtras O and Jensen H J Aa 2000 *J. Chem. Phys.* **113** 7790
[18] Carravetta V and Jansik B 2006 unpublished
[19] Okada K and Iwata S 2000 *J. Chem. Phys.* **112** 1804
[20] Botting S K and Lucchese R R 1997 *Phys. Rev.* A **56** 3666